Implementation of a 6 × 6 Free-Space Optical Fiber Ribbon Switch for Storage Area Networks

Hsi-Hsir Chou, F. Zhang, T. D. Wilkinson, N. Collings, and W. A. Crossland

***Abstract*—A shutter-based free-space optical switching architecture capable of multicast transmission functionality has been proposed as a promising switching technology for storage area network applications. The main idea behind this type of switching architecture is that the system performance can be enhanced with a new electro-optical material, used for the shutters to increase switching speed. It can be distinguished from previous shutter-based optical switches which have been based on single channel to single channel switching, as we present a reconfigurable design of a 6 × 6 72-channel shutter-based optical switching core based on multimode fiber ribbon to multimode fiber ribbon switching. The design and implementation of a prototype 6 × 6 72-channel multimode fiber ribbon switch demonstrator utilizing a submicrosecond PLZT-based spatial light modulator as a shutter is reported. The light loss, crosstalk, and data switching characteristics of the implemented fiber ribbon switch from the evaluation tests were measured and are presented.**

***Index Terms*—Fiber ribbons, free-space optical switch, lead lanthanum zirconate titanate (PLZT), spatial light modulator (SLM), storage area networks (SANs).**

I. Introduction

STORAGE area networks (SANs) have been widely implemented using optical fiber technologies since they are expected to continue to expand at ever increasing data rates in the future, due to increased storage demands from commercial enterprise and personal entertainment. The high-speed parallel optical link systems (such as the PAROLI [1]) offer network designers a simple means to interconnect various components for data aggregation and improvement of service in highly flexible and scalable networks. Multimode fiber (MMF) ribbons terminated with mechanical transferable (MT)-type connectors in conjunction with inexpensive vertical cavity surface emitting laser (VCSEL) arrays provide an optimal solution for use in high-speed market areas such as SANs, creating very short reach interfaces and input/output (I/O) to I/O interconnections [2]. In current switching technology developments, all signals transmitted over different fibers of the same fiber ribbon can only be switched separately. Moreover, there are no optical switches capable of fiber ribbon switching in today's optical switching market. This encourages the development of a fiber ribbon switch for SAN applications by switching multiple fibers together as a group in a fiber ribbon; the complexity of the switch can be significantly reduced while the bandwidth and throughput can be enhanced.

Free-space optical switching architectures such as holographic beam steering [3], [4] and shutter-based optical crossbars [5]–[7] have been proposed as promising switching technologies for constructing optical SANs [8] since traditional electronics-based switches have struggled to keep pace with SAN growth and optical fiber transmission technologies. The majority of holographic beam-steering switches use a dynamic computer-generated hologram (CGH) with a tunable periodicity controlled by a computer, displayed on a liquid crystal (LC) spatial light modulator (SLM) to direct the beams into the desired output ports. Holographic beam-steering switches do not suffer power penalties from an optical fan-out mechanism but they have difficulty achieving scalability suitable for enhancing SAN performance. A shutter-based free-space optical switching architecture is selected for fiber ribbon switch implementation over other switching architectures as it has the ability for multicast transmission, (a prerequisite for SAN switches, as the data in SANs are often from a common source/destination [8]).

In a shutter-based optical switching architecture, the optical fan-out mechanism is performed through the use of a fixed CGH-based binary phase grating (BPG) element to duplicate the optical input beam onto an SLM which acts as an array of shutters to select one or a subset of the beams for propagation to the output fiber ports [9], [10]. The multicast function is very easy to achieve by modifying the shutter control algorithm to open several shutters simultaneously. Fast switching speeds of the order of micro- and submicrosecond are also possible using a Pockels effect lead lanthanum zirconium titanate (PLZT) or ferroelectric *LC* SLM [8].

In this paper, we demonstrate a reconfigurable 6 × 6 group (a total of 72 channels) optical fiber ribbon to a fiber ribbon switch based on shuttered free-space optical switching architecture for SAN applications. The proposed work as illustrated in Fig. 1 is distinguished from previous optical switches [5]–[7], [10]–[12] which were based on single channel to single channel switch matrix. This system uses groups of fibers within each ribbon as the basis set for the fiber to fiber ribbons switching. This permits the transmission of data coming from six different locations to six destinations as a group within the same switching architecture. This paper is organized as follows. Section 2 first describes the design and implementation of the proposed optical fiber ribbon switch. The experimental system performance measurement and data transmission tests are analyzed in Section 3 followed by the conclusion in Section 4.

Manuscript received November 22, 2010; revised May 25, 2011, December 21, 2011; accepted February 03, 2012. Date of publication February 22, 2012; date of current version April 06, 2012. This work was supported in part by the U.K. Engineering and Physical Sciences Research Council Department of Trade and Industry LINK project.

The authors are with the Center for Advanced Photonics and Electronics, Department of Engineering, Cambridge University, Cambridge, CB3 0FA, U.K. (e-mail: hsi-hsir.chou@trinity.cantab.net; fz208@hotmail.com; tdw13@cam.ac.uk; nc229@cam.ac.uk; wac1001@cam.ac.uk).

Color versions of one or more of the figures in this paper are available online at http://ieeexplore.ieee.org.

Digital Object Identifier 10.1109/JLT.2012.2188778

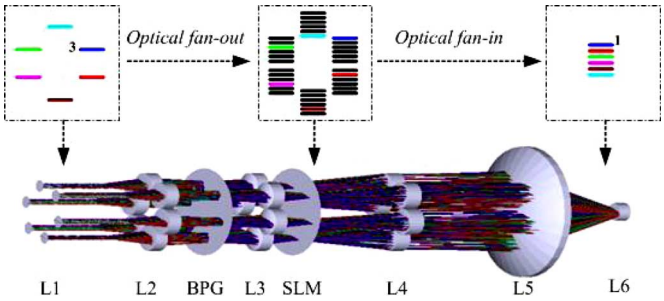

Fig. 1. Architecture and operating principle of the 6 × 6 fiber ribbon switch.

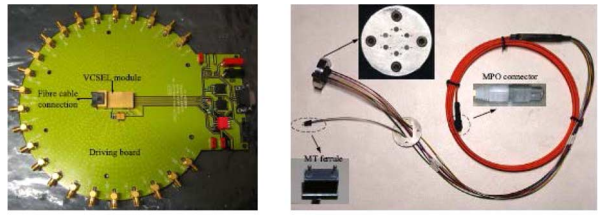

(a) (b)

Fig. 2. VCSEL transmitter and input fiber ribbons. (a) ZARLINK VCSEL transmitter module and the driving board. (b) Six input fiber ribbons terminated with MT type connectors.

II. Design and Implementation of a Fiber Ribbon Switch

In our experimental work, the switching architecture of a 6 × 6 optical fiber ribbon switch as illustrated in Fig. 1 was designed to realize data exchange between six input and six output fiber ribbons each of which transmits data arriving from six different locations to six destinations, as a group. For example, the third input fiber ribbon is going to be switched to the first output fiber ribbon position. It is duplicated six times in the shutter plane. Then the corresponding shutter at top right switches OFF the other five copies and leaves the first one ON. The signals transmitted by the third input fiber ribbon are now directed to the first output fiber ribbon through the fan-in optics. The fiber ribbons were arranged hexagonally in the input plane of the switch as illustrated in Fig. 1, to reduce optical aberrations since the biggest advantage of the hexagonal arrangement was that the symmetry of the hexagonal pattern about the center compared with a regular 2 × 3 array arrangement in which the asymmetry of relative to the center means that the fiber ribbons located each of the six different positions of the array will experience different aberrations, which results in large positional errors. The hexagonal architecture effectively improved the coupling accuracy and further improved the coupling efficiency and transmission performance. Moreover, from the simulation results using the ZEMAX software to compare the focus performance of the generated spots, it was clear that both the focused spot sizes and the spot positions generated by the hexagonal arrangement of the switching architecture had better performance than a regular 2 × 3 array arrangement. The whole switching system design and implementation according to Fig. 1 can be divided into four parts: input fiber ribbons and optical transmissions; optical fan-out subsystem; PLZT SLM; lens system (L1–L6) and optical fan-in subsystem. Of these four parts, all lenses are commercially available while the BPG element and the PLZT SLM were custom designed within the project and fabricated at external foundries.

A. Input Fiber Ribbons and Optical Transmissions

In the switching architecture as illustrated in Fig. 1, six input fiber ribbons launched by VCSELs were arranged hexagonally (VCSEL array providing optical signals for input fiber ribbons) and each fiber ribbon then used an MT connector style optical package to mount 12 MMFs (62.5 μm) in a row with a 250 μm spacing between the centers of adjacent fibers. A 12 × 2.7 Gb/s parallel fiber optic link transmitter (ZL60101) provided by ZARLINK semiconductor Inc. [13] was used as shown in Fig. 2(a). This transmitter had a 12-channel 850 nm VCSEL array interfaced with an industry standard MPO (multifiber push on) ribbon fiber connector. It provided 12 parallel channels with each channel transmitting data at a rate up to 2.7 Gb/s. The six input fiber ribbons were obtained by splitting a single 12-channel fiber ribbon launched by the VCSEL transmitter into six parts. Each part had two fibers terminated with a 12-channel MT ferrule as shown in Fig. 2(b). Six 12-channel MT-type connectors of six 2-channel fiber ribbons were positioned in the input plane. Since the hexagonal architecture as discussed previously was used in the switching system, the six input fiber ribbons were arranged as a hexagon and each fiber ribbon had a microlens array attached to its surface as shown in Fig. 2(b). These fiber ribbons were held by a custom-designed holder to ensure the precise position of each ribbon connector.

B. Optical Fan-Out Subsystem

The fan-out subsystem includes the BPG element and six separate 4f systems. A BPG element was used within a 4f optical system between L2 and L3 to perform optical fan-out, which was a replication of each input fiber ribbon onto the SLM. The design of a computer-generated BPG element was initiated by specifying the locations of the spots on a pixelated grid, separated by a distance of p pixels. The actual distance between spots on the reply field SLM (Fourier plane) is determined by the formula [14]:

$$d = \frac{\lambda \cdot f \cdot p}{\Delta \cdot N} \tag{1}$$

where λ is the wavelength of light source, f is the focal length of the Fourier lens (L3), d is the actual spot spacing, Δ is the actual size of a pixel, and N is the number of pixels along one dimension of the CGH, which is one period of the BPG. In the proposed switching system, in order to implement 6 × 6 channel switching, a BPG element capable of generating six spots in row, i.e., 1 × 6 spot pattern was required. The wavelength λ used was 850 nm; Δ and N were selected based on previous design experience ($\Delta = 10$ μm, $N = 64$); the actual spot spacing d was then determined by f and p. The spot size generated by the BPG element was 62.5 μm, i.e., equal to the diameter of a 62.5 μm MMFs and the actual PLZT SLM pixel width was 200 μm (pixel gap is 50 μm), to ensure that all spots were located on the PLZT SLM pixels; hence, the maximum allowable spot spacing d was 277.5 μm and the minimum allowable spacing was 222.5 μm. Under these constraints, a value of $p = 10$ and $f = 20$ mm was selected. Six pairs of small achromatic lenses made up of these 4f systems were arranged in a hexagon. These lenses were held in custom-designed holders. Fig. 3(a) shows the BPG element held in the holder and Fig. 3(b) shows the framed lens arrays of L2, L3, and L4.

In order to understand the characteristics of the actual grating, measurements were performed using the knife-edge method [15]. A Honeywell HFE4085 lensed 850 nm VCSEL was used as the light source for providing sufficient light power

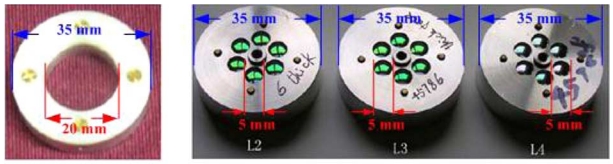

(a) (b)

Fig. 3. Components of the optical fan-out subsystem. (a) Grating element. (b) Lens arrays held by custom-designed lens holders.

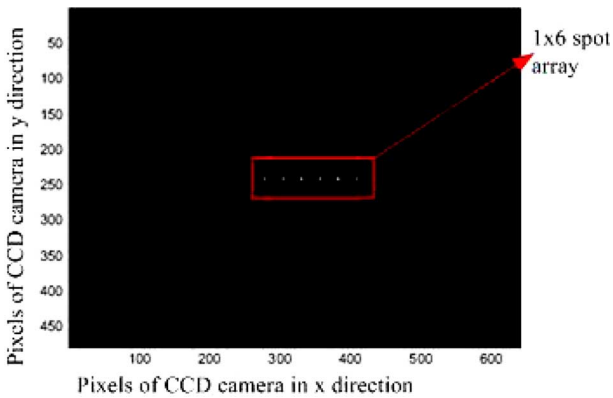

Fig. 4. 1×6 spot patterns generated by BPG element.

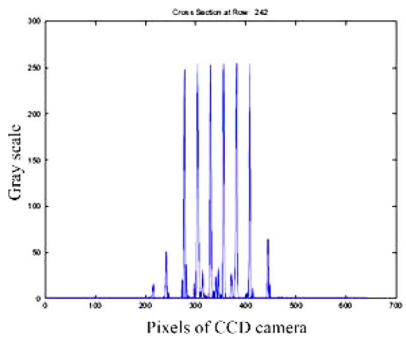

Fig. 5. Spot profile analyzed by using MATLAB.

for the grating measurement. Since the minimum step of the available micrometer was 10 μm, there was a 10 μm measurement error. The average spot size at full-width half-maximum was measured as 25 μm$\pm$10 μm and the spot diameter at 10% of maximum was 33.3 μm$\pm$10 μm. The measured spot spacing was 255 μm$\pm$10 μm. The diffraction efficiency was measured as 70%. The difference between the measured and the designed results were caused by fabrication errors. Because the BPG element was not coated, the reflection of the glass also resulted in a 10% light loss. The spot pattern generated by the BPG element was also recorded by a high-resolution charge coupled device (CCD) camera, as shown in Fig. 4. The pixel size of the CCD array was 8.6 μm $\times$ 8.3 μm. The spot patterns were analyzed to get spot profiles using MATLAB, as shown in Fig. 5. The spot diameter at 10% of maximum was calculated based on the spot profiles as 32.6 μm$\pm$8.6 μm and spot spacing was 250 μm$\pm$8.6 μm.

C. SLM Design Using PLZT Material

The SLM is a vital component of shutter-based optical switches since its properties significantly determine the whole switching performance. Many materials have been studied and can potentially be used to act as SLMs. Some examples are electro-optic (EO) materials, LCs, magneto-optic materials, acoustic-optic and photo-refractive materials. Of these materials, PLZT has been widely used as shutters, filters, and displays. The fast response, high resolution, and wide operating temperature range make PLZT a viable candidate for the SLM [16]. The PLZT material consists of a wide range of homogeneous compositions existing within the basic lead zirconate (Zr)-lead titanate (Ti) solid solution system. The general formula describing the compositions La/Zr/Ti $(x, y, 1-y)$ in the PLZT system is given by [17], [18]

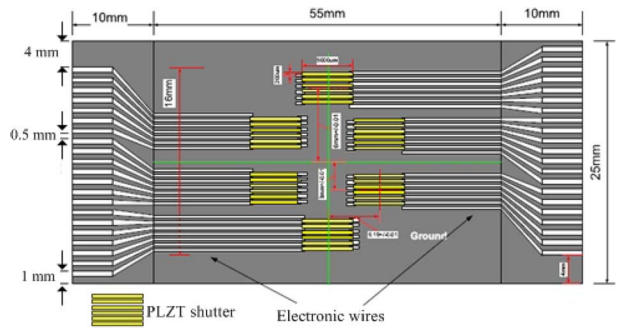

Fig. 6. Mask of six PLZT shutters.

$$Pb_{1-x}\mathrm{La}_x(\mathrm{Zr}_y Ti_{1-y})_{1-x/4}O_3. \tag{2}$$

The PLZT compositions are normally expressed by the ratio of La/PbZrO3/PbTiO3. The 65/35 ratio compositions of PbZrO3/PbT iO3 are most transparent in the La range from 8 to 16 atom percent [16]. PLZT-based devices with compositions of 8.8–9.5/65/35 are widely used in a variety of optoelectronic applications including optical switches [18], optical shutters [19], high-speed scanning, dynamic lenses, and eye-protection devices [20]. The La/Zr/Ti composition of the PLZT used in our design was equal to 9/65/35. We chose to use PLZT 9/65/35 for the shutter SLMs because of its large quadratic EO coefficient and broadband optical transmission range. The mask of the actual PLZT SLM used in the switching system is shown in Fig. 6. There are six PLZT shutters in the SLM. Each shutter has six pixels. Dimensions of each pixel are 200 μm in width, 300 μm in depth, and 5000 μm in length. The PLZT pixels have electrodes on their side faces, which are glued to each PLZT pixel to give a 250 μm pixel separation.

In order to use the PLZT as an EO switch, the PLZT SLM had to be placed between a polarizer and analyzer to realize amplitude modulation. The polarization of the input light was at an angle of 45° with respect to the long or short axis of the PLZT pixels. The external voltage was applied to rotate the incoming light polarization so that the light could pass through the analyzer. The main disadvantage of the PLZT shutters is that a high operating voltage ($\sim$150 V) was required to reach the full ON state. Despite this, contrast ratios in excess of 5000: 1 can be achieved because of the good OFF state (0.0007%) produced with a high efficiency polarizer. We defined the rise (fall) time as the time taken for the detected intensity to change from 10% (90%) to 90% (10%). The rise time decreased with increasing applied electric field. Under an applied voltage of 120 V, the rise time of the PLZT SLM was as illustrated in Fig. 7, 1 μs. A

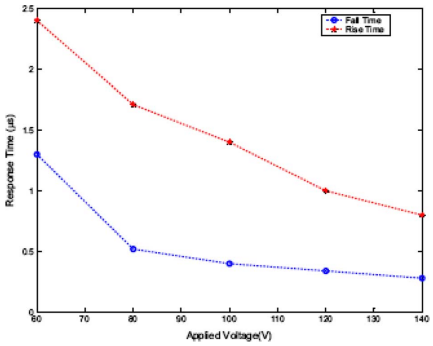

Fig. 7. PLZT response time and applied voltage.

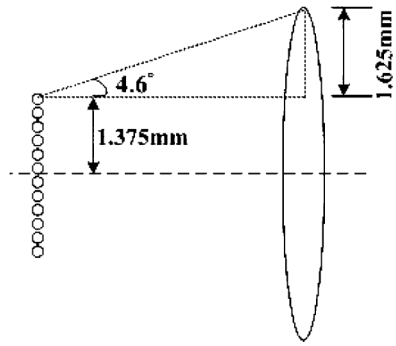

Fig. 8. Edge channel position of an input fiber ribbon.

shorter rise time can be achieved with greater voltages. However, the probability of electrical breakdown is increased. Thus, the maximum voltage applied was limited to 150 V.

D. Lens System (L1–L6) and Optical Fan-In Subsystem

The aim of the lens system design within the switching system was to find a set of suitable lenses to satisfy multiple stringent demands: imaging the input fiber ribbons onto the SLM shutters and making sure that all spots were located in the shutter pixels; focusing light onto the receiving plane and coupling the light into the receiving fibers with minimum light loss and minimum crosstalk. The lens system must be of unit magnification since the input fiber ribbons and the output fiber ribbons were all ended with commercially available MT-type connectors which have 12 fibers in a row with 250 μm spacing between the centers of two adjacent fibers. Moreover, as the lens system was not an ordinary imaging system, the shape of the image was less important than the size and the position of the image, i.e., spots. Therefore, the lens selection had to consider spherical aberration and coma because of their effects on the spot size and the spot position. From our design, the lens system used includes six 4f systems composed of six pairs of lenses (L2 and L3), a set of fan-in lenses (L4 and L5), and two micro-lens arrays (L1 and L6).

In the input plane, each fiber ribbon had 12 channels, and therefore, the edge channel had an offset of 1.375 mm from the axis as illustrated in Fig. 8, and the radius of the first collimating lens (L2) was 3 mm. According to geometrical optics, the divergence angle of the light emitted by the input fiber should be less than 4.6° in order to avoid light clipping. However, the numerical apertures (NAs) of standard 50 μm and 62.5 μm MMFs were 0.2 and 0.275, respectively, which meant that with this angle, the light rays would be clipped by the lenses. To solve this problem, single-mode fibers which have a smaller NA were considered but their transmitted power would be much lower than MMFs. Therefore, a microlens array (L1) was used in front of the input fiber ribbons which were attached to the MT guide pin without any other alignment and matching glue.

Following the microlens array, six independent 4f systems composed of six pairs of lenses (L2 and L3) in conjunction with the BPG element were used for the fan-out function. The selection of lenses L2 and L3 was limited by the BPG element design as mentioned previously but also by the focusing performance of lens L5. Since lens L5 should have the capability to focus the light coming from the same position of each fiber ribbon into the corresponding fiber of the output fiber ribbon, spherical aberration of lens L5 has a significant effect on this focusing function. In order to reduce the aberration, all incoming rays to L5 should

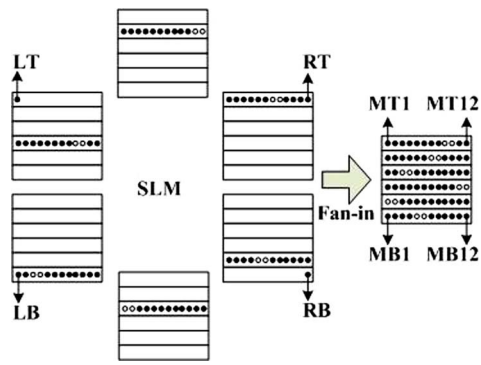

Fig. 9. Illustration of biggest coupling angle happens at optical fan-in.

be as close as possible to the optical axis. Thus, it requires the diameters of lens L2 and L3 (the position of the six shutters are determined by L2's and L3's dimension and layout) to be as small as possible, with the condition that their NAs match so as to reduce light loss. Among the commercially available achromat lenses, a lens with the diameter of 6 mm and the effective focal length (EFL) of 20 mm satisfied these conditions.

The unit magnification of the switching system determined that lens L4 and L5 should have the same EFL. As L2, L3, and L4 were coaxial, the diameter of lens L4 was also 6 mm. It was obvious that the diameter of lens L5 had to be at least three times 6 mm, i.e., 18 mm, to avoid clipping light rays. However, each light ray had a divergence angle and in order to reduce the aberrations, the diameter of L5 should be much bigger than 18 mm. It was chosen to be 30 mm. Among all commercially available lenses, a multisurface achromat and a GRADIUM lens satisfied the trade-off between the size and the EFL. Because of more light loss caused by a multisurface achromat, the GRADIUM lens was selected.

Since the NA of the output fiber ribbons was 0.275, it required that the coupling angle should be less than 16° and the coupling spot size to be less than 62.5 μm. However, in the proposed optical switching system, the biggest coupling angle was 17.5°, which occurred when fiber "LT" was coupled to fiber "MB12" or "RT" to "MB1" and fiber "LB" was coupled to fiber "MT12" or "RB" to "MT1" as illustrated in Fig. 9. The light rays coming from this angle could not be coupled into the output fibers, and consequently, light loss was caused by this mismatch of the edge channels. To solve these problems, a microlens array (L6) was used before the output fiber ribbons to reduce the coupling angle. The spot analysis results from the ZEMAX simulation showed that both the spot sizes and the spot positions were greatly improved by using the microlens array. The maximum

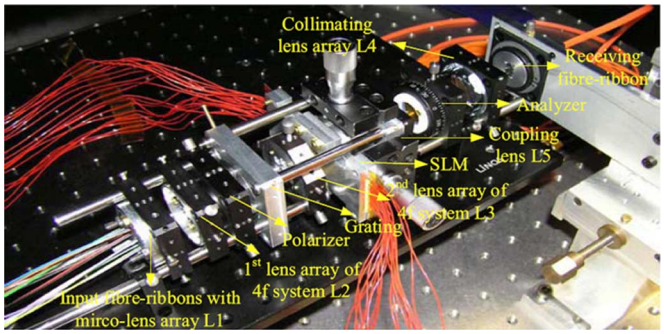

Fig. 10. Demonstrator of 6 × 6 72-channel optical fiber ribbon switch.

TABLE I
PARAMETERS OF LENS COMPONENTS

	Focal Length	Diameter	Material	Manufacturer
L1	0.63 mm	0.24 mm	Plastic	Omron
L2& L3	20 mm	6 mm	SFL6, LAKN22	Edmund Optics
L4	30 mm	6 mm	SFL6, LAKN22	Edmund Optics
L5	30 mm	30 mm	G22FN	Light Path
L6	0.5 mm	0.24 mm	Plastic	Omron

spot RMS radius (left edge fiber) is 9.97 μm and the maximum spot position error was 14 μm (for the right edge fiber). Even in these extreme cases, the spots could be projected into the fiber's receiving area totally. However, the alignment error was a major difficulty when using the microlens array. In order to achieve the results presented, the positional tolerance of the microlens array was ± 5 μm. All the lenses used in the switching system are listed in Table I.

III. Optical Switching System Performance Measurement and Analysis

The 6 × 6 72-channel optical fiber ribbon switch was experimentally implemented as illustrated in Fig. 10. The measurement and analysis of the system light loss, system crosstalk, and data switching test are presented in the following sections.

A. Performance Analysis of Optical Switching System

Although most of the custom-designed optomechanical holders were made as precisely as possible, slight errors could not be avoided because of manufacturing limitations. The manufacturing errors finally affected the focused performance in the output plane. Therefore, precise alignment was essential for a free-space optical switching system to maintain a reliable data transmission. Photographs are the most straightforward way to evaluate the working principle of the implemented optical switching system and the photos are also the best method for doing alignment, especially when an infrared wavelength is used. From our experimental work, the images of the light pattern on the key planes of the switching system were captured by a CCD camera as shown in Fig. 11. For each fiber ribbon, only the two central fibers were illuminated since a single 12 laser source was used. The illuminated fibers were used to assist alignment and evaluate the switching principle. In Fig. 11, the brighter spots mean that the lasers were in binary "1" state

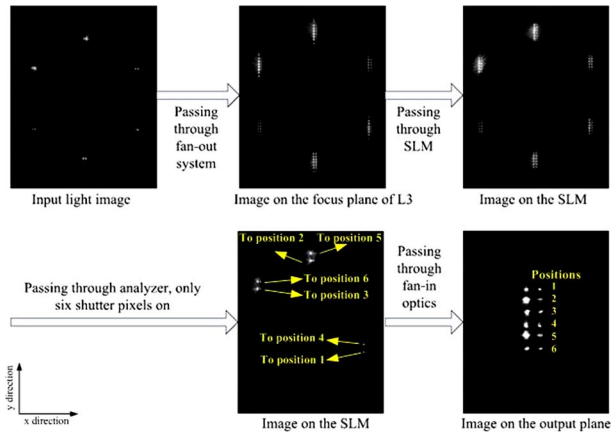

Fig. 11. Spot patterns on the key planes of a fiber ribbon switch.

and the weakest spots mean that the lasers were in binary "0" state. The lasers in an average state generated all the other spots. The top-left picture in Fig. 11 shows the input image. The top-middle picture shows the image in the focal plane of the lens L3 after the input light was replicated six times by the BPG element. By placing the PLZT SLM in the focal plane, the higher order spots were blocked. The top-right picture shows the image with the designed spots only. The two pictures at the bottom of Fig. 11 illustrate the fan-in function. These two pictures also exhibit the multicasting.

The images of the light pattern on the key planes of the switching system captured by the CCD camera were analyzed with MATLAB. The holder of the lens L3 was found to have the biggest error of 78.25 μm as exhibited in Fig. 12(a). The other holders had slight alignment errors less than 20 μm which was within the manufacturing tolerance. The joint effect of the input fiber ribbon holder and the lens array holders for L2 and L3 was reflected on the images in the SLM plane as shown in Fig. 12(b). After optimal alignment, the focused spot error measured in the experiment was 2.3% at 850 nm, which was close to the defined tolerance. In an optical transmission system, light losses usually result in a signal-to-noise ratio degradation and, thus, increase the bit error rate (BER). The majority of the components in the optical switching system are lens components, except the BPG element and PLZT SLM device. The lens components were antireflection coated and all have a theoretical transmittance of 99% according to the datasheet of the manufacturers. However, the reflection loss experienced from the lens components fabricated on the specially designed optomechanical holders and mounts was still significant due to the number of elements used in the system. The light loss caused by the optical components in the switching system was measured using a wide area power meter (Newport 1830C) and are presented in Table II.

The NA mismatch of multimode input fiber ribbon and lens L2 would result in a minimum of 5 dB light loss, and therefore, a 1 × 12 microlens array provided by Omron Electronics Components was attached directly onto the MT guide pin of each input fiber ribbon to reduce the light-beam divergence. However, the use of this microlens array resulted in a 1.2 dB insertion loss. The design efficiency of the BPG element was 84% and the measured experimental efficiency was 70%. Since the BPG element

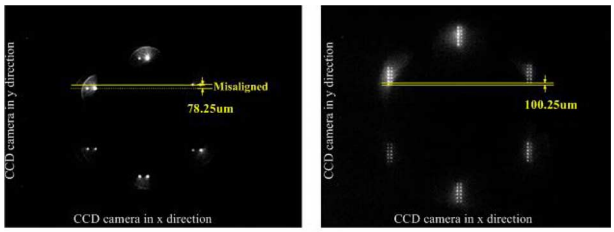

(a) (b)

Fig. 12. Analysis of spot alignment error. (a) Misaligned spots on the L3 focus plane. (b) Misaligned spots on the SLM.

TABLE II
SYSTEM LIGHT LOSS

Components	Light loss(dB)	Comments
Micro-lens array L1	1.3	Insertions & Reflections
Lens L2	0.4	Reflections
BPG element	2	Diffraction efficiency 70% Reflections:10%
Lens L3	0.4	Reflections
Fan-out	7	Power split among six spots non-uniformly
PLZT SLM & Polarizers	2.5	Transmission loss
Lens L4 & L5	1.1	Reflections & Light Clipping
Fiber Coupling	5.8	NA mismatch, spot size>fiber core
Total	20.5	

was not coated, the reflection and absorption of the glass also produced a 10% light loss resulting in a total grating loss of 2 dB. In the switching system design, the input fiber ribbon was duplicated six times by the BPG element but only one image was used when performing the switching function; hence, there was a 5/6 light loss (fan-out loss). However, if the fiber ribbon switch performs multicast transmission, then there will be less fan-out loss as all the duplicated images on the PLZT SLM could be projected into the corresponding output fiber ribbons. The polarizer and analyzer have a good transmittance (99%), and measurement results have shown that the insertion loss of the polarizer and analyzer along with PLZT SLM with in the fiber ribbon switch was around 2.5 dB. The free-space coupling into the fibers caused a light loss mainly due to the larger focused spot size than the fiber core and focusing position error. Theoretically, the use of a microlens array before the receiving fiber core would increase fiber coupling efficiency. However, from our experimental work, this was not so practical due to alignment difficulties and, therefore, resulted in a light loss of around 5.8 dB in our fiber ribbon switch.

The crosstalk of the optical switching system defined as in (3) is the ratio of the power from all other inputs to the power at the target output from the desired input

$$C_T = 10\log_{10}\left(\frac{p_n}{p_t}\right)(\text{dB}) \tag{3}$$

where p_n is the power from all other inputs and p_t is the power from the desired input. The quoted system crosstalk is usually the worst case crosstalk over all outputs. In the current switching system, the finite PLZT SLM contrast ratio, large focused spot size, and error in the focused position all resulted in crosstalk. In this system, the worst case occurred when the light sent to the target output came from the weakest spot of the six spots generated by the BPG element and all other spots around the target output were transmitting the brightest light. The light power was measured by an optical power meter Anritsu ML9001A with an FC fiber interface. The measured crosstalk was -21.7 dB. This is an acceptable figure for the SAN application as the number of users and distance of transmission are limited by the SAN and neither crosstalk nor loss are as important as the ability to do fast optical reconfiguration, especially when multicasting is available within the switch.

B. Optical Switching Performance Tests

In order to explore the switching characteristics of the optical fiber ribbon switch, the performance measurement of the optical switching system was performed at two different switching speeds: microsecond ($\sim$1 μs) switching speed in which a voltage of 120 V was applied to drive the PLZT SLM and submicrosecond switching speed ($\sim$0.5 μs) in which a voltage of 140 V was applied to drive the PLZT SLM. Since the targeted application of the fiber ribbon switch was designed for short-range SAN applications in which Gigabit Ethernet (GbE) or fiber channel has been widely deployed, switching speeds of around a microsecond are more than sufficient for the typical types of reconfigurations used in SANs. Data are not switched in these applications at the data rate, rather it is switched between data exchange packet streams or connection requests and conversations. In the optical system with multicast transmission function, the spots generated by the BPG element on the PLZT SLM plane were all projected into the output fiber core through the optical fan-in subsystem. However, in the optical system with the switching function, only selected spots on the PLZT SLM plane were projected into output fiber core and unwanted spots on the PLZT SLM plane were blocked by the PLZT SLM.

The setup for the switching performance measurement was that input pseudorandom coded data with a probability of a '1' and '0' transmission being equal were generated by a pulse pattern generator (Anritsu MP1650A). The electrical data signal went into the VCSEL module and was transmitted as optical signals. The optical signals went through the free-space optical fiber ribbon switch and entered the output fiber ribbons. The output fibers were connected to a photo-receiver, a Newfocus 1544B. Because of the weak power of the received optical signals, an HP amplifier 8447E was used after the photo-receiver. The output of the amplifier went through a low-pass filter connected to an oscilloscope (HP 54120B). From the observation of the eye diagrams, we can estimate the BER of the switch directly through the Q-factor given by [21]

$$\text{BER} = \frac{1}{2}\text{erfc}\left(\frac{Q}{\sqrt{2}}\right) \approx \frac{\exp(-Q^2/2)}{Q\sqrt{2\pi}} \tag{4}$$

where Q-factor is expressed as

$$Q = \frac{I_1 - I_0}{\sigma_0 + \sigma_1} \tag{5}$$

where I_1 and I_0 are the means of the amplitude histograms at logic one and logic zero levels, respectively. σ_0 and σ_1 are the standard deviations of the amplitude histograms at logic zero and logic one levels, respectively.

According to the measurement data shown on the eye diagrams in Fig. 13, the calculated Q-factor at microsecond switching speed was 7.04, and the estimated BER was

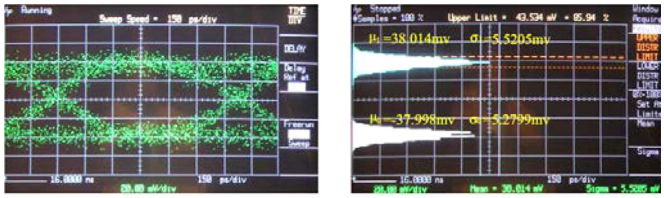

(a) (b)

Fig. 13. Microsecond switching performance at GbE link. (a) Eye diagram. (b) Histogram.

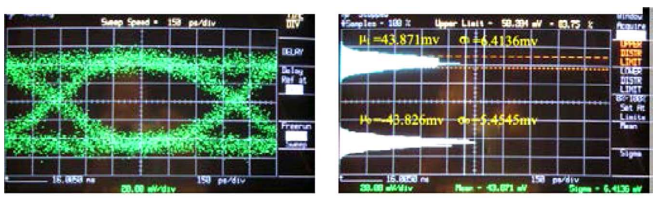

(a) (b)

Fig. 14. Submicrosecond switching performance at GbE link. (a) Eye diagram. (b) Histogram.

9.76×10^{-13} According to the measurement data shown on the eye diagrams in Fig. 14, the calculated Q-factor at submicrosecond switching speed was 7.39, and the estimated BER was 7.38×10^{-14}.

IV. Conclusion

Shutter-based free-space optical switching technology is a promising optical switching technology for constructing SANs due to its inherent capability of multicast transmission which is an important function in SAN applications. To provide data storage, an SAN has to be accessed by thousands of clients simultaneously routinely and the data transmission routing in SANs is a known quantity with self-similar statistical properties. In this paper, we have reported a new shutter-based free-space optical switch core based on an MMF ribbon to MMF ribbon switching architecture. A 6×6 72-channel MMF ribbon switch utilizing a PLZT SLM acting as a shutter, capable of submicrosecond switching speeds has been experimentally implemented and demonstrated. The implementation of the fiber-ribbon switch demonstrated, for the first time, that multichannel optical signals transmitted in the same fiber-ribbon can be switched in unison. Compared with single fiber switching, that has been dominant in optical network research, fiber-ribbon switching provides better performance for applications such as optical SANs. Furthermore, an optical switch demonstrator using multiple wavelength operation per fiber based on the same shutter-based optical switching architecture has been proved successfully recently at our research lab, meaning that such a switch could also be used for wavelength-dependent SAN solutions as well. This provides a promising future approach for the proposed fiber ribbon switch to raise its switching throughput even further and to achieve an enhanced switching capacity dramatically in the near future.

References

[1] H. Karstensen, L. Melchior, V. Plickert, K. Drogemuller, J. Blank, T. Wipiejewski, H.-D. Wolf, J. Wieland, G. Jeiter, R. Dal'Ara, and M. Blaser, "Parallel optical link (PAROLI) for multichannel gigabit rate interconnections," in *48th IEEE Electron. Compon. Technol. Conf.*, May 25–28, 1998, pp. 747–754.

[2] P. L. Pondillo, "Use of multimode fiber and 850 nm VCSEL arrays for high-speed parallel interconnects," in *14th Annu. Meet. IEEE Lasers Electro-Opt. Soc.*, 2001, vol. 2, pp. 841–842.

[3] W. A. Crossland, I. G. Manolis, M. M. Redmond, K. L. Tran, T. D. Wilkinson, M. J. Holmes, T. R. Parker, H. H. Chu, J. Croucher, V. A. Handerek, S. T. Warr, B. Robertson, I. G. Bonas, R. Franklin, C. Stace, H. J. White, R. A. Woolley, and G. Henshall, "Holographic optical switching: the "Roses" demonstrator," *J. Lightw. Technol*, vol. 18, no. 12, pp. 1845–1854, Dec. 2000.

[4] D. C. O'Brien, G. E. Faulkner, T. D. Wilkinson, B. Robertson, and D. G. Leyva, "Design and analysis of an adaptive board-to-board dynamic holographic interconnect," *Appl. Opt.*, vol. 43, pp. 3297–3305, 2004.

[5] H. White, C. Stace, M. J. Birch, A. C. Walker, M. R. Taghizadeh, T. J. Hall, and W. A. Crossland, "SLM-based optical crossbars based on the matrix-matrix principle," in *IEE Colloq. Opt. Switch.*, pp. 2/1–2/7, Digest No. 1993/137.

[6] R. W. A. Scarr, J. R. Collington, W. A. Crossland, and M. P. Dames, "Highly parallel optics in ATM switching networks," in *IEE Proc. Optoelectron.*, 1997, vol. 144, pp. 53–60.

[7] C. W. Wilmsen, C. Duan, J. R. Collington, M. P. Dames, and W. A. Crossland, "Vertical cavity surface emitting laser based optoelectronic asynchronous transfer mode switch," *Opt. Eng.*, vol. 38, pp. 1216–1222, 1999.

[8] T. D. Wilkinson, B. Crossland, N. Collings, F. Zhang, and M. Fan, "Reconfigurable free-space optical cores for storage area networks," *IEEE Commun. Mag.*, vol. 43, no. 3, pp. 93–99, Mar. 2005.

[9] R. W. A. Scarr, J. R. Collington, W. A. Crossland, and M. P. Dames, "Highly parallel optics in ATM switching networks," in *IEE Proc. Optoelectron.*, 1997, vol. 144, no. 2, pp. 53–60.

[10] A. R. Dias, R. I'. Kalman, J. W. Goodman, and A. A. Sawchuk, "Fiber-optic crossbar switch with broadcast capability," in *Proc. Int. Soc. Opt. Eng.*, 1987, vol. 825, pp. 170–177.

[11] H. J. White, G. M. Proudley, C. Stace, N. A. Brownjohn, A. C. Walker, M. R. Taghizadeh, B. R. Robertson, C. P. Barrett, W. A. Crossland, J. R. Brocklehurst, M. J. Birch, M. Snook, and D. Vass, "Development of an optical free-space crossbar," in *Proc. Opt. Comput., Inst. Phys. Conf. Ser.*, Edinburgh, U.K., 1994, vol. 139, pp. 183–186.

[12] W. A. Crossland, R. J. Mears, S. T. Warr, and R. W. A. Scarr, "Spatial-light-modulator based routing switches," in *Proc. Opt. Comput. Inst. Phys. Conf. Ser.*, 1994, vol. 139, pp. 177–182.

[13] [Online]. Available: Http://www.zarlink.com

[14] V. N. Morozov, J. A. Neff, H. Temkin, and A. S. Fedor, "Analysis of a three-dimensional computer optical scheme based on bidirectional free-space optical interconnects," *Opt. Eng.*, vol. 34, pp. 523–534, 1995.

[15] D. Wright, P. Greve, J. Fleischer, and L. Austin, "Laser beam width, divergence and beam propagation factor—an international standardization approach," *Opt. Quantum Electron.*, vol. 24, pp. S993–S1000, 1992.

[16] G. H. Haertling, "PLZT electrooptic materials and applications—A review," *Ferroelectrics*, vol. 75, pp. 25–55, 1987.

[17] Y. Sampei, S. Naito, and Y. Kurita, "PLZT fiber-optic switch," *J. Lightw. Technol.*, vol. LT-5, no. 9, pp. 1203–1206, Sep. 1987.

[18] T. Utsunomiya, "Optical switch using PLZT ceramics," *Ferroelectrics*, vol. 109, pp. 235–240, 1990.

[19] M. J. Landry and A. E. McCarthy, "Transmission switching characteristics of PLZT shutters," *Appl. Opt.*, vol. 12, no. 10, pp. 2312–2319, 1973.

[20] P. E. Shames, P. C. Sun, and Y. Fainman, "Modeling of scattering and depolarizing electro-optic devices I. Characterization of lanthanum-modified lead zirconate titanate," *Appl. Opt.*, vol. 37, no. 17, pp. 3717–3725, Jun. 1998.

[21] G. P. Agrawal, *Lightwave Technology: Telecommunication System*. New York: Wiley, 2005.

Author biographies not included at authors' request due to space constraints.